

Effect of angular momentum distribution on gravitational loss-cone instability in stellar clusters around massive BH

E. V. Polyachenko,^{1*}, V. L. Polyachenko,¹ I. G. Shukhman,^{2†}

¹*Institute of Astronomy, Russian Academy of Sciences, 48 Pyatnitskaya St., Moscow 119017, Russia*

²*Institute of Solar-Terrestrial Physics, Russian Academy of Sciences, Siberian Branch, P.O. Box 291, Irkutsk 664033, Russia*

Accepted Received

ABSTRACT

Small perturbations in spherical and thin disk stellar clusters surrounding massive a black hole are studied. Due to the black hole, stars with sufficiently low angular momentum escape from the system through the loss cone. We show that stability properties of spherical clusters crucially depend on whether the distribution of stars is monotonic or non-monotonic in angular momentum. It turns out that only non-monotonic distributions can be unstable. At the same time the instability in disk clusters is possible for both types of distributions.

Key words: Galaxy: centre, galaxies: kinematics and dynamics.

1 INTRODUCTION

Study of the gravitational loss-cone instability, a distant analog of the plasma cone instability, has begun from V. Polyachenko (1991) work in which a simplest analytical model of thin disk stellar cluster has been employed. The interest to the problem of stability of stellar clusters has been revived recently by detailed investigation by Tremaine (2005) and Polyachenko, Polyachenko, Shukhman, (2007; henceforth, Paper I) of low mass clusters around massive black holes. The both papers have considered stability of small amplitude perturbations of stellar clusters of disk-like and spherical geometry.

Tremaine (2005) has shown using Goodman’s (1988) criterion that thin disk with a symmetric DF over angular momentum and empty loss cone are generally unstable. On the contrary, analyzing perturbations with spherical numbers $l = 1$ and $l = 2$, he deduced that spherical clusters with monotonically increasing DF of angular momentum should be generally stable.

In Paper I, however, we have demonstrated that spherical systems with non-monotonic distributions may be unstable for sufficiently small-scale perturbations $l \geq 3$, while the harmonics $l = 1, 2$ remain stable. For the sake of convenience, we have used two assumptions. The first one is that Keplerian potential of the massive black hole dominates over a self-gravitating potential of the stellar cluster (which does not mean that one can neglect the latter). Then the characteristic time of system evolution is of the order of the orbit precessing time, which is slow compared to typical dynamical (free fall) time. Since a star makes many rotations in its almost unaltered orbit, we can regard it as to be “smeared

out” along the orbit in accordance with passing time, and study evolution of systems made of these extensive objects.

The second assumption is a so called *spoke approximation*, in which a system consists of near-radial orbits only. This approximation was earlier suggested by one of the authors (Polyachenko 1989, 1991). The spoke approximation reduces the problem to study of rather simple analytical characteristic equations controlling small perturbations of stellar clusters.

There are two questions that naturally arise in this context. First: Does the instability remain when abandoning the assumption of strong radial elongation of orbits? Second: Does the instability occur in spheres with monotonically increasing distributions in angular momentum if one consider smaller-scale perturbations with $l \geq 3$? The aim of the paper is to provide answers to these questions.

To achieve the task we use semi-analytical approach based on analysis of integral equations for slow modes elaborated recently in Polyachenko (2004, 2005) for thin disks, and in Paper I for spherical geometry. Following Paper I, we shall restrict ourselves to studying monoenergetic models with DFs in the form

$$F(E, L) = A \delta(E - E_0) f(L). \quad (1.1)$$

Models are specified by certain functions $f(L)$. The dependence on energy assumed in (1.1) allows us to advance greatly in analytical calculations and obtain simpler one-dimensional integral equations for determining eigenfrequencies. At the same time we suggest that the choice of energy dependence of DF in the (1.1) is unimportant for establishing stability or instability *per se* for each specific distribution under consideration.

Section 2 is devoted to spheres, Section 3 – to thin disks with symmetric DF. The sections are organized similarly. In the beginning we derive integral equations for initial distri-

* E-mail: epolyach@inasan.ru

† E-mail: shukhman@iszf.irk.ru

bution functions in the form (1.1). Then follow analytical and numerical investigations of these equations. We demonstrate that in the contrast to the case of near-Keplerian sphere, the loss-cone instability in disks takes place even for monotonic DF, $df/d|L| > 0$, provided the precession is retrograde and the loss cone is empty: $f(0) = 0$. Sec. 2 is complimented by stability analysis of models with circular orbits, which of course doesn't belong to the class of monoenergetic models of (1.1) type.

In the last, Section 4, we discuss the results and some perspectives of further studies.

2 SPHERICAL SYSTEMS

2.1 Integral equation for slow modes in monoenergetic models

For the near-Keplerian systems, the slow integral equations, which has been derived in our Paper I (see there Eq. (4.8)), are neatly suited. In contrast to Paper I, we shall not assume here strong elongation of orbits, i.e. we shall go beyond the spoke approximation.

Since energies of all stars are identical, the unperturbed DF depends on one variable only. It is convenient to use a dimensionless angular momentum $\alpha = L/L_{\text{circ}}(E_0)$, where L_{circ} is the moment at the circular orbits: $L_{\text{circ}}(E_0) = GM_c/(2|E_0|)^{1/2}$, M_c is the central point mass, G is the gravitational constant. The frequency of star radial oscillations $\Omega_1(E_0) = (2|E_0|)^{3/2}/(GM_c)$ and the radius of the system $R(E_0) = GM_c/|E_0|$ are independent of the angular momentum. For shorthand notations, we shall omit the argument E_0 .

The normalization constant A is taken so that a mass of the spherical system surrounding the central mass is equal to M_G (we assume the ratio $\epsilon \equiv M_G/M_c$ to be small: $\epsilon \ll 1$):

$$M_G = \int f d\Gamma = 2(2\pi)^3 \int \frac{dE}{\Omega_1(E)} \int_0^{L_{\text{circ}}} L dL f(E, L).$$

If one defines the normalization of the dimensionless DF as $\int_0^1 d\alpha \alpha f(\alpha) = 1$, then

$$A = \frac{\Omega_1 M_G}{16\pi^3 L_{\text{circ}}^2}. \quad (2.1)$$

It allows to represent the kernel of the integral equation (formula (4.8) in the Paper I) in the form

$$P_{s,s'}^{(l)}(E, L; E', L') = \frac{8\pi^2 (2l+1)}{R} C_l \mathcal{K}_{s,s'}^{(l)}(\alpha, \alpha'),$$

where l is the index of the spherical harmonic, $C_l = \int_0^\infty dz z^{-1} [J_{(l+1)/2}(z) J_{l/2}(z)]^2$ and $J_\nu(z)$ is the Bessel function.¹ The functions $\mathcal{K}_{s,s'}^{(l)}$ satisfy to the condition

¹ For $l = 1$ the coefficient C_1 can be calculated analytically: $C_1 = 4/3\pi^2 \approx 0.135$. Numerical calculations show decreasing C_l with increasing the mode number l : $C_2 = 0.063$, $C_3 = 0.0373$, $C_4 = 0.025$, $C_5 = 0.018$, and so on.

$\mathcal{K}_{s,s'}^{(l)}(0, 0) = 1$; their explicit form is given later. Then substitution of DF in the form (1.1) leads to the following integral equation:

$$\phi_s(\alpha) = 16\pi^3 G A R C_l \sum_{s'=s_{\min}}^l s'^2 D_l^{s'} \times \int_0^1 \frac{\Omega_{\text{pr}}(\alpha') \alpha' df(\alpha')/d\alpha'}{\omega^2 - s'^2 \Omega_{\text{pr}}^2(\alpha')} \mathcal{K}_{s,s'}^{(l)}(\alpha, \alpha') \phi_{s'}(\alpha') d\alpha', \quad (2.2)$$

where $\phi_s(\alpha)$ is the Fourier harmonics of the radial part of the perturbed potential (for more detail, see Paper I), $\Omega_{\text{pr}}(\alpha)$ is the orbital precession rate, $s_{\min} = 1$ for odd l , and $s_{\min} = 2$ for even l . The coefficients D are calculated by the formula

$$D_l^s = \begin{cases} \frac{1}{2^{2l}} \frac{(l+s)!(l-s)!}{\left[\left(\frac{1}{2}(l-s)\right)!\left(\frac{1}{2}(l+s)\right)!\right]^2}, & |l-s| \text{ even,} \\ 0 & |l-s| \text{ odd.} \end{cases} \quad (2.3)$$

By changing the unknown function $[\omega^2 - s^2 \Omega_{\text{pr}}^2(\alpha)] \times \varphi_s(\alpha) = \phi_s(\alpha)$, Eq. (2.2) can be reduced to the linear eigenvalue problem

$$[\omega^2 - s^2 \Omega_{\text{pr}}^2(\alpha)] \varphi_s(\alpha) = 16\pi^3 G A R C_l \sum_{s'=s_{\min}}^l s'^2 D_l^{s'} \times \int_0^1 \Omega_{\text{pr}}(\alpha') \alpha' \frac{df(\alpha')}{d\alpha'} \mathcal{K}_{s,s'}^{(l)}(\alpha, \alpha') \varphi_{s'}(\alpha') d\alpha'. \quad (2.4)$$

For the almost radial orbits, when $\alpha \ll 1$ or eccentricity $e \equiv \sqrt{1 - \alpha^2} \approx 1$, the precession rate is

$$\Omega_{\text{pr}}(\alpha) = -\frac{2\epsilon \Omega_1}{\pi^2} \alpha [1 + O(\alpha^2)]. \quad (2.5)$$

For the orbits with smaller eccentricity the numerical coefficient preceding the small parameter $\epsilon \Omega_1$ is somewhat greater than $2/\pi^2$. Since one suggests that the characteristic frequencies of the problem under consideration are of the order of typical precession velocities, $\omega \sim \Omega_{\text{pr}} \sim \epsilon \Omega_1$, it is convenient to change to the dimensionless frequencies, measured in natural “slow” units:

$$\bar{\omega} = \frac{\omega}{\epsilon \Omega_1}, \quad \nu(\alpha) = -\frac{\Omega_{\text{pr}}(\alpha)}{\epsilon \Omega_1}. \quad (2.6)$$

For the spherical systems the precession is retrograde (see Tremaine 2005, or Paper I), so $\nu(\alpha) > 0$. Then the dimensionless integral equation becomes

$$[\bar{\omega}^2 - s^2 \nu^2(\alpha)] \varphi_s(\alpha) = -2 C_l \sum_{s'=s_{\min}}^l s'^2 D_l^{s'} \times \int_0^1 \nu(\alpha') \alpha' \frac{df(\alpha')}{d\alpha'} \mathcal{K}_{s,s'}^{(l)}(\alpha, \alpha') \varphi_{s'}(\alpha') d\alpha', \quad (2.7)$$

For obtaining the eigenfrequency spectrum for a model, it is necessary to compute preliminarily the kernels $\mathcal{K}_{s,s'}^{(l)}(\alpha, \alpha')$ (universal for all models), and the precession rate profile $\nu(\alpha)$ for the given model. When integrating over

Keplerian orbits, it is most convenient to turn to the variable τ that is connected with the current radius r and the true anomaly ζ of a star² by the following formulas:

$$r = \frac{1}{2}(1 - e \cos \tau), \quad \cos \zeta = \frac{\cos \tau - e}{1 - e \cos \tau}. \quad (2.8)$$

Then after some transformations, the kernel $\mathcal{K}_{s,s'}^{(l)}$ can be reduced to the form

$$\mathcal{K}_{s,s'}^{(l)}(\alpha, \alpha') = \frac{2}{(2l+1)\pi^2 C_l} \int_0^\pi d\tau r \cos(s\zeta) \times \int_0^\pi d\tau' r' \cos(s\zeta') \mathcal{F}_l(r, r'), \quad (2.9)$$

where r' and ζ' specify the position of a star on the orbit with the eccentricity e' corresponding to the variable τ' , and the notation

$$\mathcal{F}_l(r, r') = \frac{\min(r, r')^l}{\max(r, r')^{l+1}}$$

is used.

The expression for the precession rate can be obtained by transformation of expression (4.2) of Tremaine (2005) (see also Paper I):

$$\nu(\alpha) = \frac{\alpha}{4\pi e} \int_0^\pi \frac{\mu(r)(\cos \tau - e) d\tau}{r^2}, \quad \nu(1) = -\frac{1}{4} \pi \rho(\frac{1}{2}). \quad (2.10)$$

For the monoenergetic models, the minimal and maximal radii are $R_{\min} = \frac{1}{2} R(1 - e_{\max})$, $R_{\max} = \frac{1}{2} R(1 + e_{\max})$, where $e_{\max} = (1 - h^2)^{1/2}$, and h is the minimal dimensionless angular momentum corresponding to the boundary of loss cone.

The function $\mu(r)$ is a ratio of the mass of a spherical system inside the sphere of radius r to the total mass M_G :

$$\mu(r) = \frac{\mathcal{M}_G(r)}{M_G}, \quad \mathcal{M}_G(r) = 4\pi \int_{R_{\min}}^r x^2 \rho(x) dx, \quad (2.11)$$

$M_G = \mathcal{M}_G(R_{\max})$, and the density is calculated by the formula

$$\rho(r) = \frac{4\pi A}{r} \int_0^{L_{\max}(r)} \frac{f(L) L dL}{\sqrt{L_{\max}^2 - L^2}} = \frac{M_G}{\pi^2 r R^2} \bar{\rho}(r), \quad (2.12)$$

$$\bar{\rho}(r) = \int_0^{\alpha_{\max}(r)} \frac{2\alpha d\alpha f(\alpha)}{\sqrt{\alpha_{\max}^2 - \alpha^2}},$$

where $\alpha_{\max} = \sqrt{4(r/R)(1 - r/R)}$. From here on we shall assume $R = 1$.

Using (2.8) and (2.10)–(2.12) one can transform the expression for the scaled precession rate $\nu(\alpha)$ to more universal form:

$$\nu(\alpha) = \frac{\alpha}{2\pi^2 e^2} \int_0^1 d\alpha' \alpha' f(\alpha') \mathcal{Q}(\alpha, \alpha'), \quad (2.13)$$

where the kernel $\mathcal{Q}(\alpha, \alpha')$ doesn't depend on DF and equals to

$$\mathcal{Q}(\alpha, \alpha') = 4 \int_{p_{\min}}^{p_{\max}} dr \sqrt{\frac{(r - r_{\min})(r_{\max} - r)}{(r - r'_{\min})(r'_{\max} - r)}}, \quad (2.14)$$

with $p_{\min} = \max(r_{\min}, r'_{\min})$, $p_{\max} = \min(r_{\max}, r'_{\max})$. Here $r_{\min} = \frac{1}{2}(1 - e)$, $r_{\max} = \frac{1}{2}(1 + e)$, $r'_{\min} = \frac{1}{2}(1 - e')$, $r'_{\max} = \frac{1}{2}(1 + e')$, and $e = (1 - \alpha^2)^{1/2}$, $e' = (1 - \alpha'^2)^{1/2}$. For the near radial orbits $\mathcal{Q}(0, 0) = 4$, so that one obtains the above mentioned result (2.5): $\nu \approx (2/\pi^2)\alpha$.

2.2 Analytical results

2.2.1 Exact solution with zero frequency for the lopsided mode ($l = 1$)

Tremaine (2005) has noted that for an arbitrary distribution $F(E, L)$ with empty loss cone, $F(E, L = 0) = 0$, a zero frequency lopsided mode $l = 1$ must exist. The mode corresponds to a non-trivial perturbation arising under shift of the spherical system as a whole relative to the central mass. The perturbed potential in such a mode is $\delta\Phi(r, \theta) = -\xi \cos \theta \frac{d\Phi_G}{dr}$, where ξ is the displacement. In terms of the function $\phi_{s=1}(\alpha)$, this perturbation has a form

$$\phi_1(\alpha) = \frac{e}{\alpha} \nu(\alpha), \quad (2.15)$$

or in terms of the function $\varphi_1(\alpha)$ from (2.7),

$$\varphi_1(\alpha) = \frac{e}{\alpha \nu(\alpha)}. \quad (2.16)$$

One can check that (2.15) and $\bar{\omega} = 0$ (provided the condition $f(0) = 0$) is a solution of (2.2) or (2.7) for $l = 1$, taking into account the expressions (2.13) and (2.14), written in the form

$$\mathcal{Q}(\alpha, \alpha') = -\frac{16}{\alpha'} \frac{\partial}{\partial \alpha'} \int_{p_{\min}}^{p_{\max}} dr \sqrt{(r - r_{\min})(r_{\max} - r)} \times \sqrt{(r - r'_{\min})(r'_{\max} - r)},$$

and also the expression for the kernel $\mathcal{K}_{11}^{(1)}(\alpha, \alpha')$

$$\mathcal{K}_{11}^{(1)}(\alpha, \alpha') = \frac{6}{e e'} \int_{p_{\min}}^{p_{\max}} dr \sqrt{(r - r_{\min})(r_{\max} - r)} \times \sqrt{(r - r'_{\min})(r'_{\max} - r)}.$$

The very existence of zero modes is crucial for stability analysis of spherical clusters with monotonic distributions. Indeed, the role of destabilizing contribution of the second term in the right side of (2.7) falls off with increasing the number l . So, it is expected that the most “dangerous” modes correspond to the lowest values of l . But it turns out that $l = 1$ mode is neutrally stable, and the next dangerous mode $l = 2$ is stable. Note, however, that this stability reasoning is valid for systems with monotonic distributions only.

² True anomaly is the angle between directions to the star and to the pericenter.

2.2.2 The stable mode in systems with near-radial orbits

By analyzing (2.7), it is easy to find one more analytical solution with the frequency $\bar{\omega} = \mathcal{O}(1)$ at arbitrary values of l , for the models with highly elongated orbits. First of all we note that the frequency of this stable mode corresponds to the resonance on the *tail* of narrow-localized distribution, and so it decays exponentially slowly. In this way the mode differ from the unstable modes of interest which have a resonance in a region where the distribution is localized, i.e. at $\alpha \lesssim \alpha_T$; so they have characteristic frequencies and growth rates of order of $\mathcal{O}(\alpha_T)$.

After setting $\bar{\omega} \sim 1 \gg \alpha_T$ in (2.7), omitting the second summand in l.h.s., turning to the spoke approximation, and taking into account the equality $\sum_{s=s_{\min}}^l s^2 D_l^s = \frac{1}{2} l(l+1)$, one finds

$$\bar{\omega}^2 = 2C_l l(l+1). \quad (2.17)$$

It is essential that this *high-frequency* mode is independent of details of DF. Note also that in the systems with prograde precession, this mode describes the well-known radial orbit instability (instead of the neutral oscillations).

2.2.3 The Variational principle

Using (2.7), one can prove two important statements:

- (i) In models of spherical systems with monotonic distributions $f(\alpha)$, the eigenfrequency squared, $\bar{\omega}^2$, must be a real number. This means that either the instability is absent at all, or aperiodic instability with $\text{Re } \bar{\omega} = 0$ occurs.
- (ii) Rotating (or oscillating) unstable modes may appear only in models with non-monotonic distributions.

Let us write Eq. (2.7) in the form

$$\begin{aligned} \bar{\omega}^2 \varphi_s(\alpha) = s^2 \nu^2(\alpha) \varphi_s(\alpha) - 2C_l \sum_{s'=s_{\min}}^l s'^2 D_l^{s'} \times \\ \times \int_0^1 g(\alpha') \mathcal{K}_{ss'}^{(l)}(\alpha, \alpha') \varphi_{s'}(\alpha') d\alpha', \end{aligned} \quad (2.18)$$

where $g(\alpha) = \nu(\alpha) \alpha df(\alpha)/d\alpha$. We multiply both parts of Eq. (2.18) by $s^2 D_l^s \varphi_s^*(\alpha)$, sum the result over s (asterisk means the complex conjugation), and integrate over α with the weight $g(\alpha)$. Then we obtain

$$\begin{aligned} \bar{\omega}^2 \int_0^1 g(\alpha) d\alpha \sum_{s=s_{\min}}^l s^2 D_l^s |\varphi_s(\alpha)|^2 = \\ = \int_0^1 \nu^2(\alpha) g(\alpha) d\alpha \sum_{s=s_{\min}}^l s^4 D_l^s |\varphi_s(\alpha)|^2 - \\ - 2C_l \int_0^1 d\alpha \int_0^1 d\alpha' \sum_{s=s_{\min}}^l \sum_{s'=s_{\min}}^l (ss')^2 D_l^s D_l^{s'} \times \\ \times \mathcal{K}_{ss'}^{(l)}(\alpha, \alpha') [g(\alpha) \varphi_s^*(\alpha)] [g(\alpha') \varphi_{s'}(\alpha')]. \end{aligned} \quad (2.19)$$

The reality of the coefficients of $\bar{\omega}^2$ in the l.h.s. of (2.19) and the first term in the r.h.s. is evident. With the help of (2.9),

one can show that the kernel in Eq. (2.19) has the following property of symmetry:

$$\mathcal{K}_{s,s'}^{(l)}(\alpha, \alpha') = \mathcal{K}_{s',s}^{(l)}(\alpha', \alpha). \quad (2.20)$$

So, one can readily see that the second term in the r.h.s. is real also. Consequently, taking the imaginary part of Eq. (2.19), one obtains

$$\text{Im}(\bar{\omega}^2) \int_0^1 g(\alpha) d\alpha \sum_{s=s_{\min}}^l s^2 D_l^s |\varphi_s(\alpha)|^2 \equiv 0. \quad (2.21)$$

From the last equality, the statements formulated above follow immediately. If the function $g(\alpha)$ (or, equivalently, $df(\alpha)/d\alpha$) is constant-sign, then the integral should be non-zero, and so $\text{Im}(\bar{\omega}^2) = 0$. In contrast, when $\text{Im}(\bar{\omega}^2) \neq 0$, the integral must be equal to zero. Consequently, the function $g(\alpha)$ should change its sign, i.e. DF $f(\alpha)$ is non-monotonic.

Let us explain the term *variational principle* used in the title of this subsection. Consider a dynamic equation in the form $d^2\xi/dt^2 \equiv -\omega^2\xi = -\hat{K}\xi$. Provided that “elasticity operator” \hat{K} is hermitian, the dynamic equation may be obtained from the conditions $\delta(\omega^2)/\delta\xi = 0$ and $\delta(\omega^2)/\delta\xi^* = 0$. Here $\delta\xi$ and $\delta\xi^*$ are considered formally as independent variations while the functional ω^2 is

$$\omega^2 = \frac{\int \xi^*(\hat{K}\xi) w(\alpha) d\alpha}{\int |\xi|^2 w(\alpha) d\alpha}$$

($w(\alpha)$ is a nonnegative weight function). In such a case it is used to speak about the variational (or energy) principle (see, e.g., review by Kadomtsev 1966 on MHD-stability of plasma). From the other hand it is easy to understand that if $\int |\xi|^2 w(\alpha) d\alpha \neq 0$ for any nontrivial ξ then ω^2 is real. Thus usually (as is a case in MHD-stability theory of plasma where \hat{K} is hermitian and $w > 0$) the notions “variational principle” and reality of ω^2 are identical. However, in our case the condition $\int |\xi|^2 w(\alpha) d\alpha \neq 0$ is not satisfied for any nontrivial ξ unless DF is monotonic. Assuming that this condition is fulfilled, following the tradition that originates from plasma physics we speak that the variational principle takes place. Only in this case the dynamical equation can be interpreted mechanically, in terms of elastic forces.

Evidently, the condition (2.21) is a serious obstacle to obtain unstable rotating modes. So, one might want to get round this obstacle. For instance, if we slightly change the initial monotonically increasing DF in a narrow region near $\alpha = 1$, to vanish quickly but smoothly, then a modified system would be practically indistinguishable from the initial one. But then the variational principle breaks down. The question can be formulated as follows: May the discontinuous vanishing $f(\alpha)$ at $\alpha = 1$ be considered as the violation of monotony for DF?

Importance of this question is known since stability study of stellar systems with isotropic DFs, $F = F(E)$ (Antonov, 1960, 1962). The variational principle there required DF to be decreasing function of energy E , $F'(E) < 0$, everywhere. The systems with $F'(E) > 0$ need separate examinations, that was carried out in some cases (see, e.g., Antonov, 1971, Kalnajs, 1972, Polyachenko and Shukhman, 1972, 1973, Fridman and Polyachenko, 1984). An essential difference of the second type of DFs is in jumps to zero at the phase space boundary $E = E_{\text{bound}}$. In fact, we have

in this case an interval degenerated into the single point $E = E_{\text{bound}}$ where $F(E)$ is decreasing.

We checked numerically a possibility of the instability connected with the edge maximum of DF over angular momentum. For this purpose, number of models smoothed near $\alpha = 1$ were computed. The computations showed no sign of instability, in contrast to isotropic distributions, $F = F(E)$. The reason for the tolerance of our present models is in fact that the kernels \mathcal{K} of integral operators in (2.18) vanish at the circular orbits, $\alpha = 1$, so details of the initial distribution near circular orbits cannot affect much solutions of the integral equation (2.18).

Roles of different terms in Eq. (2.18) can be easily followed. When $\partial F / \partial L > 0$, the first term of the right side in Eq. (2.18) favors stabilization, while the second term gives destabilization (taking into account that the operator involved into this construction is self-adjoint and positively defined). In principle, this destabilizing effect could lead to instability. However, this is not the case because the stabilizing contribution exceeds destabilizing one in all cases considered both by Tremaine (2005) and in the present paper (see the following sections).

2.3 Unstable models

Instability boundaries in terms of the angular momentum dispersion $\alpha_T < (\alpha_T)_c$ found in Paper I for monoenergetic DF with

$$f(\alpha) = \frac{N}{\alpha_T^2} \left(\frac{\alpha^2}{\alpha_T^2} \right)^n \exp(-\alpha^2/\alpha_T^2), \quad (2.22)$$

(N is the normalization constant, α_T is the dimensionless angular momentum dispersion, n is the real number) have a qualitative character only: formally, these boundaries lie outside the validity of the spoke approximation, since $(\alpha_T)_c \sim 1$. Obtaining such critical dispersions means only that the spoke models, in which $\alpha_T \ll 1$ by definition, are certainly unstable. So the quantitative determination of these boundaries with help of the exact integral equation is required. The *power-exp* model (2.22) is studied in Sec. 2.3.1.

In Sec. 2.3.2 we study a simplest *Heaviside* model consisting of two steps (at $\alpha = h_1$ and at $\alpha = h_2$) (both in the spoke approximation framework and using exact integral equation):

$$f(\alpha) = \frac{2}{h_2^2 - h_1^2} \left[H(\alpha - h_1) - H(\alpha - h_2) \right], \quad h_1 < h_2 < 1 \quad (2.23)$$

($H(\alpha)$ denotes the Heaviside function). Finally, in Sec. 2.3.3. we consider the *log-exp* model with DF

$$f(\alpha) = \frac{N}{\alpha_T^2} \ln(\alpha^2/h^2) \exp(-\alpha^2/\alpha_T^2), \quad (2.24)$$

for $\alpha \geq h$, and $f(\alpha) = 0$ for $\alpha < h$, i.e., with the empty loss cone (N is the normalization constant).

2.3.1 The power-exp model

Following Paper I, here we consider the stability of models (2.22) with $n = 2$ and $n = 3$ relative to the spherical harmonic $l = 3$. We remind that at the limit $\alpha_T \ll 1$, both these

models were unstable (the stability boundaries obtained using spoke approximation were $(\alpha_T)_c = 0.193$ for $n = 2$, and $(\alpha_T)_c = 0.283$ for $n = 3$).

For distribution (2.22) one finds

$$N^{-1} = \frac{1}{2} \int_0^{1/\alpha_T^2} x^n \exp(-x) dx.$$

Particularly, in the case $\alpha_T \ll 1$, the normalization constant is $N = 2/(n!)$. From (2.12), we obtain

$$\bar{\rho}(r) = N \int_0^{\alpha_{\text{max}}^2(r)/\alpha_T^2} \frac{z^n e^{-z} dz}{\sqrt{\alpha_{\text{max}}^2 - z \alpha_T^2}}.$$

Further calculations of the density (2.12) and precession rate (2.13) profiles should be evaluated numerically.

Solutions of the integral equation (2.7) for $n = 2$ and $n = 3$ show similar behavior. At small values of α_T , each model has one unstable mode. With increasing the dimensionless angular momentum dispersion α_T , the growth rate of the instability decreases, and then vanishes at some critical value $(\alpha_T)_c$: for the model $n = 2$, $(\alpha_T)_c^{(2)} \simeq 0.301$, for the model $n = 3$, $(\alpha_T)_c^{(3)} \simeq 0.311$ (see Fig. 1). We conclude that the spoke approximation in this case is qualitatively correct, but quantitatively poor. The instability becomes saturated at some critical value $(\alpha_T)_c$, while the discrepancy of $(\alpha_T)_c$ values between exact and approximate values for both models are not small.

Apart from the unstable mode, the spectrum of each model has a discrete mode, the growth rate of which is equal to zero at small values of α_T , and becomes negative with increasing α_T . This is just that weakly decaying mode with the frequency $\bar{\omega}^2 \approx 2C_l l(l+1)$ (at $\alpha_T \ll 1$) which was mentioned in Sec. 2.2.2. The dependence of the frequency on l for this mode was one of tests for numerical code of the integral equation solver. Another test consisted in detecting the zero lopsided mode $l = 1$ mentioned in Sec. 2.2.1.

The third test was the evaluation of $\bar{\omega}(\alpha_T)$ dependence in the spoke approximation limit. Assuming that $\bar{\omega} = 2\lambda\alpha_T/\pi^2$, and using $\mathcal{K}_{s,s'}^{(l)}(\alpha, \alpha') \approx 1$, $\phi_s(\alpha) \approx 1$, and $\nu(\alpha) \approx 2\alpha/\pi^2$ in (2.2), one can obtain the equation for the $l = 3$ mode

$$\int_0^\infty dz (n - z) z^n e^{-z} \left(\frac{1}{\lambda^2 - z} + \frac{1}{\lambda^2 - 9z} \right) = 0. \quad (2.25)$$

This equation has one unstable mode for each n : $\lambda = 4.98 + 0.88i$ for $n = 2$, and $\lambda = 6.18 + 2.88i$ for $n = 3$. The same values obtained from solution of the exact integral equation (2.7) are $\lambda = 4.97 + 0.82i$ and $\lambda = 6.4 + 2.73i$, correspondingly.

2.3.2 The Heaviside model

The simplest non-monotonic model that allows to progress rather far by analytical methods is the model with a piecewise constant distribution over momentum (2.23). In other words, we assume the DF to be non-zero only within the interval $h_1 < \alpha < h_2$, where it is taken constant.

When studying stability of discontinuous distributions such as (2.23), it is more convenient to start with the integral

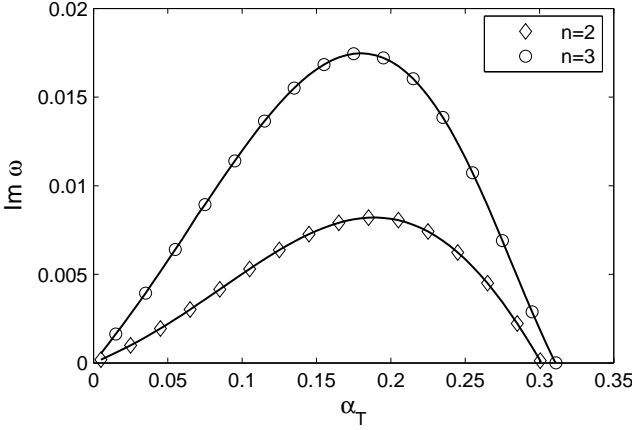


Figure 1. The dependence of the growth rate $\text{Im}(\bar{\omega})$ vs. dimensionless angular momentum dispersion α_T of the mode $l = 3$ for models $n = 2$ (diamonds) and $n = 3$ (circles). Dashed line show the asymptotic behavior obtained using spoke approximation equation (2.25).

equation in the form (2.2). Substituting (2.23) into Eq. (2.2), one obtains

$$\begin{aligned} \phi_s(\alpha) = & \frac{4C_l \epsilon \Omega_1}{h_2^2 - h_1^2} \sum_{s'=s_{\min}}^l s'^2 D_{s'}^l \left[\frac{\Omega_{\text{pr}}(h_1) h_1}{\bar{\omega}^2 - s'^2 \Omega_{\text{pr}}^2(h_1)} \times \right. \\ & \times \mathcal{K}_{ss'}^{(l)}(\alpha, h_1) \phi_{s'}(h_1) - \frac{\Omega_{\text{pr}}(h_2) h_2}{\bar{\omega}^2 - s'^2 \Omega_{\text{pr}}^2(h_2)} \times \\ & \left. \times \mathcal{K}_{ss'}^{(l)}(\alpha, h_2) \phi_{s'}(h_2) \right]. \quad (2.26) \end{aligned}$$

Let us turn again to the natural slow scale of frequencies according (2.6) and then substitute in (2.26) particular values $\alpha = h_1$ and $\alpha = h_2$. For brevity sake, we introduce the denotations $\nu_1 \equiv \nu(h_1)$, $\nu_2 \equiv \nu(h_2)$. We have

$$\begin{aligned} \phi_s(h_1) = & -\frac{4C_l}{h_2^2 - h_1^2} \sum_{s'=s_{\min}}^l s'^2 D_{s'}^l \left[\frac{\nu_1 h_1}{\bar{\omega}^2 - s'^2 \nu_1^2} \mathcal{K}_{ss'}^{(l)}(h_1, h_1) \times \right. \\ & \left. \times \phi_{s'}(h_1) - \frac{\nu_2 h_2}{\bar{\omega}^2 - s'^2 \nu_2^2} \mathcal{K}_{ss'}^{(l)}(h_1, h_2) \phi_{s'}(h_2) \right], \quad (2.27) \end{aligned}$$

$$\begin{aligned} \phi_s(h_2) = & -\frac{4C_l}{h_2^2 - h_1^2} \sum_{s'=s_{\min}}^l s'^2 D_{s'}^l \left[\frac{\nu_1 h_1}{\bar{\omega}^2 - s'^2 \nu_1^2} \mathcal{K}_{ss'}^{(l)}(h_2, h_1) \times \right. \\ & \left. \times \phi_{s'}(h_1) - \frac{\nu_2 h_2}{\bar{\omega}^2 - s'^2 \nu_2^2} \mathcal{K}_{ss'}^{(l)}(h_2, h_2) \phi_{s'}(h_2) \right]. \quad (2.28) \end{aligned}$$

This set of equations relative to $\phi_s(h_1)$ and $\phi_s(h_2)$, ($s = 1, 2, \dots, [\frac{1}{2}(l+1)]$) can be reduced to the standard linear set. Introducing new unknown functions

$$X_s = \frac{\nu_1 h_1}{\bar{\omega}^2 - s^2 \nu_1^2} \phi_s(h_1), \quad Y_s = \frac{\nu_2 h_2}{\bar{\omega}^2 - s^2 \nu_2^2} \phi_s(h_2),$$

one obtains

$$\begin{aligned} (\bar{\omega}^2 - s^2 \nu_1^2) X_s = & -4C_l \frac{\nu_1 h_1}{h_2^2 - h_1^2} \sum_{s'=s_{\min}}^l s'^2 D_{s'}^l \times \\ & \times \left[\mathcal{K}_{ss'}^{(l)}(h_1, h_1) X_{s'} - \mathcal{K}_{ss'}^{(l)}(h_1, h_2) Y_{s'} \right], \quad (2.29) \end{aligned}$$

$$\begin{aligned} (\bar{\omega}^2 - s^2 \nu_2^2) Y_s = & -4C_l \frac{\nu_2 h_2}{h_2^2 - h_1^2} \sum_{s'=s_{\min}}^l s'^2 D_{s'}^l \times \\ & \times \left[\mathcal{K}_{ss'}^{(l)}(h_2, h_1) X_{s'} - \mathcal{K}_{ss'}^{(l)}(h_2, h_2) Y_{s'} \right]. \quad (2.30) \end{aligned}$$

The precession rates in these equations can be expressed through the complete elliptical integrals \mathbf{K} and \mathbf{E} :

$$\nu_1 = 2C_1 \frac{h_1}{e_1} \frac{1 - q^2 Q(q)}{1 - q^2}, \quad \nu_2 = 2C_1 \frac{h_2}{e_1} \frac{Q(q) - q}{1 - q^2},$$

where $C_1 = 4/(3\pi^2)$, $q = e_2/e_1$, $e_1 = (1 - h_1^2)^{1/2}$, $e_2 = (1 - h_2^2)^{1/2}$, and the function $Q(q)$ is

$$Q(q) = \frac{1}{2q^2} \left[(1 + q^2) \mathbf{E}(q) - (1 - q^2) \mathbf{K}(q) \right].$$

In the limit $h_2 \rightarrow h_1$, the frequencies ν_1 and ν_2 are coincident: $\nu_1 = \nu_2 = (2/\pi^2)(h/e)$, where $h = h_1 = h_2$, and $e = e_1 = e_2$. Note that a determinant of the set of equations (2.29) and (2.30) has a rank $2[\frac{1}{2}(l+1)]$. Particularly, for the mode $l = 1$, the rank is equal to 2. Roots of the determinant are calculated numerically. The difference $h_2 - h_1$ has a meaning of dispersion, i.e., it is analogous to the parameter α_T in our models with smooth distributions.

A simple analytical task is to ascertain that $\bar{\omega}^2 = 0$ is the eigenvalue of the determinant for $l = 1$. We have for $\mathcal{K}_{11}^{(1)}(\alpha, \alpha')$

$$\mathcal{K}_{11}^{(1)}(\alpha, \alpha') = e < Q(\kappa), \quad (2.31)$$

where $\kappa = e < /e >$, $e < = \min(e, e')$, $e > = \max(e, e')$, $e = (1 - \alpha^2)^{1/2}$, $e' = (1 - \alpha'^2)^{1/2}$. In particular,

$$\mathcal{K}_{11}^{(1)}(h_1, h_1) = e_1, \quad \mathcal{K}_{11}^{(1)}(h_2, h_2) = e_2, \quad (2.32)$$

$$\mathcal{K}_{11}^{(1)}(h_1, h_2) = \mathcal{K}_{11}^{(1)}(h_2, h_1) = e_2 Q(q), \quad q = e_2/e_1. \quad (2.33)$$

Setting $\bar{\omega}^2 = 0$ in the determinant of the set (2.29) and (2.30), and using the expressions for the elements of the kernel (2.32) and (2.33), we can show that it is equal to zero identically. This just means the occurrence of a zero mode in the spectrum. Another root $\bar{\omega}^2$ for $l = 1$ is positive for any values of h_1 and h_2 , which agrees with our previous conclusion (Paper I) that the instability is absent for the mode $l = 1$.

It is useful to derive equations in (2.29) and (2.30) in the spoke limit, when the distribution is localized in a region of small values of α . This means that we suggest $h_1 \ll 1$, $h_2 \ll 1$, $h_1 < h_2$, set in (2.26) $\phi_s(\alpha) = (-1)^s$, $\mathcal{K}_{ss'}^{(l)} = (-1)^{s+s'}$, and finally obtain

$$1 = -\frac{4C_l}{h_2^2 - h_1^2} \sum_{s=s_{\min}}^l s^2 D_s^l \left[\frac{\nu_1 h_1}{\bar{\omega}^2 - s^2 \nu_1^2} - \frac{\nu_2 h_2}{\bar{\omega}^2 - s^2 \nu_2^2} \right]. \quad (2.34)$$

For the precession frequencies ν_1 and ν_2 , one has in this limit $\nu_1 = (2/\pi^2) h_1$, $\nu_2 = (2/\pi^2) h_2$. Introducing $\bar{\omega} = \frac{1}{2}\pi^2 \bar{\omega}$, let us write down, e.g., the characteristic equation for the mode $l = 3$. In this case $D_1^3 = \frac{3}{16}$, $D_3^3 = \frac{5}{16}$, hence

$$\begin{aligned} 1 = & -\frac{3\pi^2 C_3}{8} \frac{1}{h_2^2 - h_1^2} \left[\frac{h_1^2}{\bar{\omega}^2 - h_1^2} + \frac{15h_1^2}{\bar{\omega}^2 - 9h_1^2} - \right. \\ & \left. - \frac{h_2^2}{\bar{\omega}^2 - h_2^2} - \frac{15h_2^2}{\bar{\omega}^2 - 9h_2^2} \right]. \quad (2.35) \end{aligned}$$

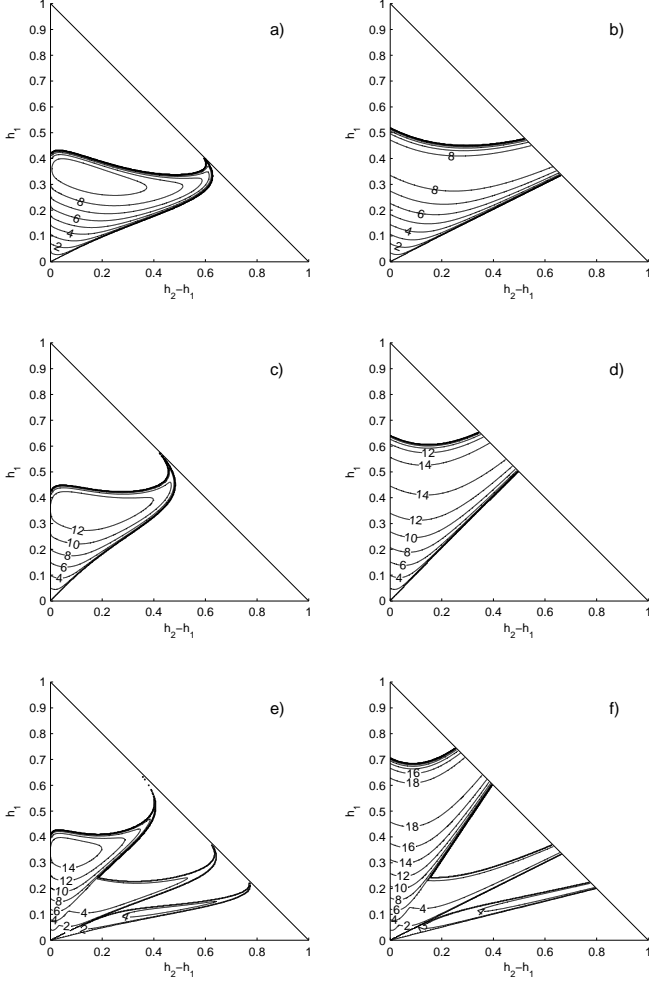


Figure 2. The stability boundaries and the isolines $10^2 \text{Im}(\bar{\omega})$ on the plane $(h_2 - h_1, h_1)$ for the Heaviside model (left: exact calculations, right: spoke approximation calculations): *a* and *b* – for the mode $l = 3$; *c* and *d* – for the mode $l = 4$, *e* and *f* – for mode $l = 5$. The spoke approximation is reliable in the lower left corner of the domain. It is also seen that for $l = 3$, the growth rate is sharply decreased when the ratio of the difference $h_2 - h_1$ (the analog of the dispersion α_T for models with smooth DFs) to the size of the loss cone, h_1 , becomes greater than 2.2.

Due to the denominator $h_2^2 - h_1^2 \approx 2(h_2 - h_1) \ll 1$, the role of “self-gravity” may be made sufficiently large in spite of small parameter C_3 . This may give the oscillating instability under certain conditions for h_1 and h_2 . The limiting solutions serves a test for the model with arbitrary h_1 and h_2 .

The results for the modes $l = 3$, $l = 4$ and $l = 5$ are presented in Fig. 2*a–f*. They show the boundaries of instability domains on the plane $(h_2 - h_1, h_1)$. Left panels show the results of computations from the exact set of equations (2.29) and (2.30); right panels – the results from the spoke equation for this model (2.34). It is seen that in the region $h_1 \ll 1$, $h_2 - h_1 \ll 1$, the results obtained from the spoke equation and those from the exact equations do coincide. Location of the growth rate maxima at Figs. 2*a*, 1*c*, 1*e*, as

well as the values of growth rates are practically the same.³ We conclude that for non-monotonic DF the instability is insensitive to a number l of the mode. This is a characteristic feature for the loss-cone instability. Recall that in models with monotonic distributions, the destabilizing term quickly decreases with increasing spherical number l of the mode. So, one may check only the lowest modes for instability.

2.3.3 The log-exp model

In some numerical models (see, e.g., Cohn, Kulsrud, 1978, Berczik et. al. 2005) the initially isotropic distribution transforms under action of a massive black hole into one monotonically increasing with angular momentum, $f(\alpha) \propto \ln(\alpha/h)$, where h defines the minimum angular momentum of a star which is not absorbed by the black hole. In this section, we consider the stability of DF (2.24). For it, one finds

$$N^{-1} = \int_h^1 \frac{d\alpha}{\alpha^2} \ln\left(\frac{\alpha^2}{h^2}\right) e^{-\alpha^2/\alpha_T^2} = \frac{1}{2} \left[-\text{Ei}(-h^2/\alpha_T^2) + \text{Ei}(-1/\alpha_T^2) + \ln(h^2) e^{-1/\alpha_T^2} \right],$$

where $\text{Ei}(z)$ is the exponential integral. Density profile is obtained from (2.12):

$$\bar{\rho}(r) = \frac{N}{\alpha_T^2} \int_{h^2}^{\alpha_{\max}^2(r)} \frac{dz}{\sqrt{\alpha_{\max}^2(r) - z}} \ln\left(\frac{z}{h^2}\right) e^{-z/\alpha_T^2}.$$

In common with the power-exp model considered above, the calculations of the precession rate should be performed numerically.

The qualitative pattern of the spectrum for this model is similar to that for the power-exp model: when the dispersion is not too large, two discrete modes occur, one of which being unstable. Comparison of the instability domains and values of growth rates in the given model and in the Heaviside model also shows qualitative coincidence of the instability patterns in dependence on the dispersion of DF and the size of loss cone.

In Fig. 3 (left panel), the isolines $10^2 \text{Im}\bar{\omega}$ on the plane of parameters (α, h) for the mode $l = 3$ are presented. The location of isolines in this model is similar to those in the Heaviside model. The right panel shows the ratio of imaginary part to real part of $\bar{\omega}$ vs. dimensionless angular momentum dispersion α_T for several values of loss cone size parameter h .

2.4 Stable models

The first consideration of possible instability of spherical clusters around massive black holes was performed by Tremaine (2005). He considered distributions of the form

$$f(I_1, I_2) \propto I_1^b \ln\left(\frac{I_2}{h I_1}\right) \quad (2.36)$$

³ Two additional instability domains for $l = 5$ are explained by more complicated structure of the characteristic equation for this mode, compared to the modes $l = 3$ and $l = 4$.

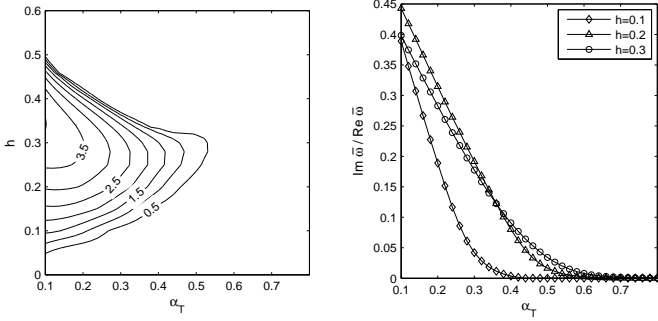


Figure 3. The mode $l = 3$ for the log-exp model. Left: isolines $10^2 \text{Im } \bar{\omega}$ on the plane (α, h) . Right: the ratio of the growth rate $\text{Im } \bar{\omega}$ to the real part of the frequency $\text{Re } \bar{\omega}$, for values $h = 0.1, 0.2, 0.3$.

in the domain $I_{\min} \leq I_1 \leq I_{\max}$, $I_2 > hI_1$ (and zero outside this domain); $I_r, I_2 = L$ are the action variables, $I_1 = I_r + L$; b and h are the real parameters. In the distribution, the loss cone is empty for dimensionless angular momentum $\alpha < h$. Tremaine studied the most large-scale perturbations with the spherical indices $l = 1$ and $l = 2$.

In this section we consider two monoenergetic models. The first one is

$$f(\alpha) = N \ln \left(\frac{\alpha^2}{h^2} \right), \quad h < \alpha < 1, \quad (2.37)$$

where $h < 1$ characterize size of the loss cone, N is the normalization constant. Dependence of distributions (2.36) and (1.1) with $f(L)$ from (2.37) on the angular momentum is identical. Just this dependence is crucial for stability or instability of each specific distribution. Stability of distribution (2.37) for arbitrary values of l is proved in Sec. 2.4.1.

Another distribution (Sec. 2.4.2) is the simplest *monotonic Heaviside* model in a form of the step-like DF,

$$f(\alpha) = \frac{2}{1-h^2} H(\alpha-h) H(1-\alpha). \quad (2.38)$$

The factor $H(1-\alpha)$ is added to reflect that the DF domain is bounded by circular orbits.

In Sec. 2.4.3, we prove the stability of spherical systems (in the field of a central massive body), all orbits of which are circular.

2.4.1 The log model

Distribution in the form (2.37) allows to calculate the density $\rho(r)$ explicitly. Using (2.12) one obtains:

$$\bar{\rho}(r) = N \int_{h^2}^{\alpha_{\max}^2(r)} \frac{d(\alpha^2)}{\sqrt{\alpha_{\max}^2(r) - \alpha^2}} \ln \left(\frac{\alpha^2}{h^2} \right), \quad (2.39)$$

where the normalization constant satisfies the relation:

$$N^{-1} = \int_h^1 d\alpha \alpha \ln \left(\frac{\alpha^2}{h^2} \right) = \frac{1}{2} \left[\ln \left(\frac{1}{h^2} \right) - (1-h^2) \right].$$

From the condition $h^2 \leq \alpha_{\max}^2(r) \equiv (4r/R)(1-r/R)$, it follows that

$$R_{\min} = \frac{1}{2} R (1 - \sqrt{1-h^2}), \quad R_{\max} = \frac{1}{2} R (1 + \sqrt{1-h^2}).$$

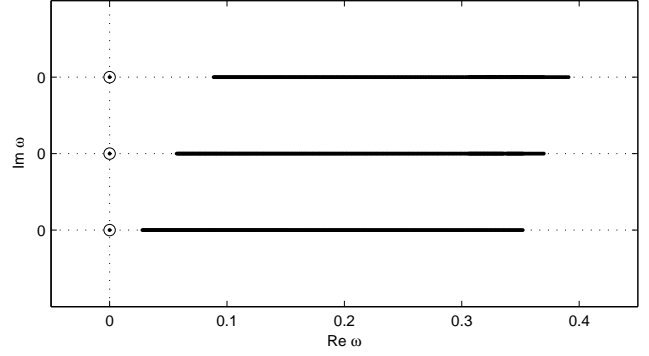


Figure 4. Spectrum for the log model with $h = 0.1, 0.2, 0.3$ for $l = 1$. In all cases the eigenfrequencies are neutral and consist of one zero mode (circled point) and continuous part of spectrum (points run into a line). To save room the spectra are shown in a single plot, but vertically separated from one another.

In presence of the loss cone, $h > 0$, the radius of the system R_{\max} is less than the apocenter radius for a radial orbit R , since stars with low angular momentum, $\alpha < h$, are absorbed by the black hole. Integration (2.39) gives for the density

$$\bar{\rho}(r) = \frac{4}{R} \left[\sqrt{r(R-r)} \times \ln \frac{\sqrt{r(R-r)} + \sqrt{(r-R_{\min})(R_{\max}-r)}}{\sqrt{R_{\min} R_{\max}}} - \sqrt{(r-R_{\min})(R_{\max}-r)} \right].$$

As is seen the density vanishes smoothly at the boundaries of the spherical layer $r = R_{\min}$ and $r = R_{\max}$. The expressions for the precession velocity are defined by the formulas (2.10)–(2.11).

In Fig. 4, the frequency spectrum, $\bar{\omega}$, of the spherical harmonic $l = 1$ for the *log*-model is presented for different values of the parameter h . All calculations detect zero modes.

For other values of l (we considered $l = 2, 3$), the discrete modes are absent in the frequency spectra at any values of h . The spectra are continuous and lie at the region of real and positive values of $\bar{\omega}^2$. We conclude that the log models are turned out to be stable.

2.4.2 The monotonic Heaviside model

Following the procedure described in Sec. 2.3.2 for the unstable Heaviside model, one can derive for (2.38) the equation:

$$\phi_s(h) = -\frac{C_l}{C_1} \frac{2}{\sqrt{1-h^2}} \sum_{s'=s_{\min}}^l D_{s'}^l \frac{s'^2}{\lambda^2 - s'^2} \mathcal{K}_{ss'}^{(l)}(h, h) \phi_{s'}(h), \quad (2.40)$$

where $\lambda = \bar{\omega}/\nu(h)$, $\nu(h) = 8h/[3\pi^2 e(h)]$. It is easy to see that for $l = 1$ there is a zero mode only, since $\mathcal{K}_{11}^{(1)}(h, h) = e(h) = (1-h^2)^{1/2}$. Introducing new variables $X_s = s \phi_s(h) \sqrt{D_s^l}/(\lambda^2 - s^2)$ one reduces (2.40) to a stan-

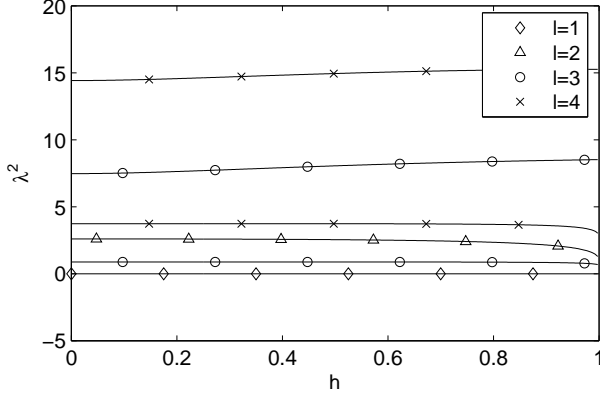


Figure 5. The dependence of the eigenfrequencies squared, $\lambda_j^2(h)$, for $l = 1, 2, 3, 4$.

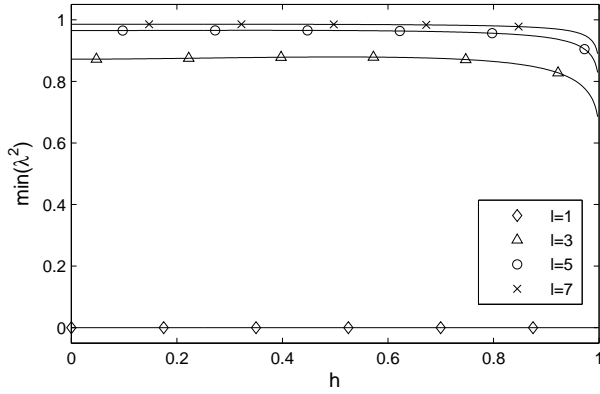


Figure 6. The dependence of the smallest (for given l) eigenfrequencies squared, $\lambda^2(h)$, for $l = 1, 3, 5$, and 7 .

linear set

$$\lambda^2 X_s = s^2 X_s - \sum_{s'=s'_{\min}}^l \hat{L}_{ss'}^{(l)}(h) X_{s'}, \quad (2.41)$$

where matrix

$$\hat{L}_{ss'}^{(l)}(h) = 2 \frac{C_l}{C_1} \frac{\mathcal{K}_{ss'}^{(l)}(h, h)}{e(h)} s s' \sqrt{D_s^l D_{s'}^l}.$$

is Hermitian. So, the eigenfrequencies λ^2 are real. Here again we have a competition of opposite factors, expressed by the first and the second terms in the r.h.s of (2.41). To conclude whether the instability occurs, we must find numerically zeros of the determinant $\|(s^2 - \lambda^2) \delta_{ss'} - \hat{L}_{ss'}^{(l)}\| = 0$, as a function of λ^2 for $l \geq 2$. A rank of the determinant is equal to $[\frac{1}{2}(l+1)]$.

The results are represented in Figs. 5 and 6. This figures show the dependence of $\lambda_j^2(h)$, $j = 1, 2, \dots, [\frac{1}{2}(l+1)]$ as a function of the loss cone size h . The instability is clearly absent. Each eigenvalue $\lambda_i^2(h)$ has only a weak dependence on h and approximately equals to j^2 . The least stable mode is $l = 3$ (see Fig. 6), but still it is far from instability.

2.4.3 Model with circular orbits

Let us consider the simplest monotonic model, in which all orbits are circular. In this section we do not assume distributions to be monoenergetic, otherwise the model degenerates into a spherical envelope. Let us assume that DF is $F(E, L) \propto \delta[L - L_{\text{circ}}(E)]$, or, in v_r and $v_\perp = \sqrt{v_\theta^2 + v_\phi^2}$ variables:

$$F(v_r, v_\perp, r) = \frac{\rho_0(r)}{2\pi v_0(r)} \delta(v_r) \delta[v_\perp - v_0(r)], \quad v_0(r) = r\Omega(r),$$

where $\Omega(r)$ is the angular velocity of a star at the circular orbit, this velocity being determined by a balance of the centrifugal force and a sum of the gravitational forces from the central body and from the spherical cluster: $\Omega^2 = \Omega_0^2(r) + (1/r) d\Phi_G(r)/dr$, $\Omega_0^2(r) = GM_c/r^3$. Here we also suggest that $\Omega_0^2 \gg r^{-1} d\Phi_G(r)/dr$.

In this approximation, the orbits are near-Keplerian, and the following relations are valid:

$$\begin{aligned} \omega_0^2 &\equiv 4\pi G\rho_0(r) = \Phi_G'' + \frac{2}{r} \Phi_G', \\ \Omega &= \Omega_0 + \frac{1}{2r\Omega_0} \Phi_G', \\ \kappa &= \Omega_0 + \frac{1}{2\Omega_0} \left(\Phi_G'' + \frac{3}{r} \Phi_G' \right). \end{aligned} \quad (2.42)$$

For the precession rate we have (see also Tremaine, 2001) $\Omega_{\text{pr}} = \Omega - \kappa = -(1/2\Omega_0) \times [\Phi_G'' + (2/r) \Phi_G']$, or, taking into account (2.42), $\Omega_{\text{pr}} = -\frac{1}{2} \omega_0^2 / \Omega_0$. Since $\epsilon = M_G/M_c \ll 1$, one has the following scalings: $\Omega_{\text{pr}} \sim \epsilon \Omega_0$, $\omega_0^2 \sim \epsilon \Omega_0^2$, and for slow modes $\omega \sim \Omega_{\text{pr}} \sim \epsilon \Omega_0$.

We start from the equation derived by Pal'chik et. al. (1970), for the models with circular orbits (the equation can also be found in the monography of Fridman and Polyachenko (1984).⁴ It has a form:

$$\frac{d}{dr} r^2 A_l(r, \omega) \frac{d\chi_l}{dr} - B_l(r, \omega) \chi_l(r) = 0, \quad (2.43)$$

where $\chi_l(r)$ is radial part of potential perturbation $\Phi(r) \propto \chi_l(r) Y_l^m(\theta, \varphi) \exp(-i\omega t)$, coefficients $A_l(r, \omega)$ and $B_l(r, \omega)$ are

$$A_l(r, \omega) = 1 + \omega_0^2 \sum_{s=-l}^l \frac{D_s^l}{[\omega - (s\Omega - \kappa)][\omega - (s\Omega + \kappa)]}, \quad (2.44)$$

$$\begin{aligned} B_l(r, \omega) &= l(l+1) + \sum_{s=-l}^l D_s^l \times \\ &\left\{ r^2 \frac{d}{dr} \left[\frac{\omega_0^2}{r} \frac{2s\Omega}{(\omega - s\Omega)(\omega - (s\Omega - \kappa))(\omega - (s\Omega + \kappa))} \right] + \right. \\ &+ \omega_0^2 \left[\frac{4s\Omega(\omega - s\Omega) + s^2[(\omega - s\Omega)^2 + 4\Omega^2 - \kappa^2]}{(\omega - s\Omega)^2 [\omega - (s\Omega - \kappa)][\omega - (s\Omega + \kappa)]} + \right. \\ &\left. \left. \frac{(l+s+1)(l-s)}{(\omega - s\Omega)(\omega - s\Omega - 2\Omega)} \right] \right\}. \end{aligned} \quad (2.45)$$

Now we need to distinguish between even and odd values of l , since l and s should be of the same parity.

⁴ Note that both in the monography and in the original paper, the form of equation does not allow to include the external gravitational field from a halo or a central body. We have slightly changed the equation to make it possible.

For even l , the dominating contributions is expected from $s = 0$ and $s = -2$. However, one can see that for even l , the contributions from $s = 0$ and $s = -2$ cancel each other. Indeed, setting $\omega_0^2 = -2\Omega_0\Omega_{\text{pr}}$:

$$A_l = 1, \quad B_l = l(l+1) + D_0^l l(l+1) \frac{\Omega_{\text{pr}}}{\Omega} - D_2^l (l-1)(l+2) \frac{\Omega_{\text{pr}}}{\Omega}.$$

Taking into account the relation

$$D_2^l = D_0^l \{l(l+1)/[(l-1)(l+2)]\},$$

one obtains: $A_l = 1$, $B_l = l(l+1)$. So the equation (2.43) is reduced to the trivial relation $\Delta\chi_l = 0$, which means the absence of the slow density perturbations.

For odd l , the main contributions into the sum for odd l comes from terms $s = \pm 1$, so one has:

$$A_l = 1 + 2D_1^l \frac{\Omega_{\text{pr}}^2}{\omega^2 - \Omega_{\text{pr}}^2},$$

$$B_l = l(l+1) - 4D_1^l r^2 \frac{d}{dr} \left(\frac{1}{r} \frac{\Omega_{\text{pr}}^2}{\omega^2 - \Omega_{\text{pr}}^2} \right). \quad (2.46)$$

To study this case we transform the differential equation (2.43) with A_l and B_l from (2.46) to an integral equation. Eq.(2.43) can be represented in the form of the Poisson equation

$$\Delta\chi_l(r) = 4\pi G\rho_l(r), \quad (2.47)$$

with the perturbed density

$$\rho_l(r) = -\frac{D_1^l}{4\pi G} \left\{ \frac{1}{r^2} \frac{d}{dr} \left[r^2 S(\omega^2, r) \frac{d\chi_l}{dr} \right] + \frac{d}{dr} \left[\frac{2}{r} S(\omega^2, r) \right] \chi_l \right\}, \quad (2.48)$$

where $S(\omega^2, r) = 2\Omega_{\text{pr}}^2/(\omega^2 - \Omega_{\text{pr}}^2)$. The solution of Eq. (2.47) in the integral form is:

$$\chi_l(r) = -\frac{4\pi G}{2l+1} \int r'^2 dr' \rho_l(r') \mathcal{F}_l(r, r') \quad (2.49)$$

where the kernel

$$\mathcal{F}_l(r, r') = \frac{(r')^l}{r^{l+1}} H(r - r') + \frac{r^l}{(r')^{l+1}} H(r' - r), \quad (2.50)$$

or, substituting (2.48) into (2.49), and integrating by parts,

$$\chi_l(r) = -\frac{D_1^l}{2l+1} \int dr' S(\omega^2, r') \frac{d}{dr'} [r'^2 \chi_l(r')] \times$$

$$\times \left[\frac{d\mathcal{F}_l(r, r')}{dr'} + \frac{2}{r'} \mathcal{F}_l(r, r') \right]. \quad (2.51)$$

Applying the operator $\hat{\mathcal{P}}(r) = d/dr + 2/r$ to both parts of Eq. (2.51) and denoting $\Psi_l(r) = \hat{\mathcal{P}}(r) \chi_l(r) = d\chi_l(r)/dr + (2/r) \chi_l(r)$ we obtain an integral equation⁵

$$\Psi_l(r) = -\frac{D_1^l}{2l+1} \int r'^2 dr' S(\omega^2, r') \mathcal{R}_l(r, r') \Psi_l(r'), \quad (2.52)$$

with the new symmetrical kernel $\mathcal{R}_l(r, r') =$

⁵ The integral equation (2.52) can also be derived from the general “slow” integral equation, by considering of circular orbit limit. However, that derivation is much more cumbersome than one given here.

$(d/dr + 2/r) (d/dr' + 2/r') \mathcal{F}_l(r, r')$. Introducing the new function $Z_l = r \Omega_{\text{pr}}/(\omega^2 - \Omega_{\text{pr}}^2) \Psi_l$, we obtain the required integral equation

$$[\omega^2 - \Omega_{\text{pr}}(r)^2] Z_l(r) =$$

$$- \frac{2D_1^l}{2l+1} \int dr' \Omega_{\text{pr}}(r) \Omega_{\text{pr}}(r') \mathcal{K}_l(r, r') Z_l(r'), \quad (2.53)$$

with the kernel $\mathcal{K}_l(r, r') = r r' \mathcal{R}_l(r, r')$.

Since the kernel defines a self-adjoint integral operator, all eigenfrequencies ω^2 should be real. To determine whether negative values of ω^2 are possible, let us write out the kernel $\mathcal{K}_l(r, r')$ explicitly:

$$\mathcal{K}_l(r, r') = -(l+2)(l-1) \mathcal{F}_l(r, r') + (2l+1) \delta(r - r'). \quad (2.54)$$

It contains two contributions: the first is negative, the second is positive. Substituting (2.54) into (2.53), one finds

$$\omega^2 Z_l(r) = \Omega_{\text{pr}}^2(r) (1 - 2D_1^l) Z_l(r) + 2D_1^l \frac{(l+2)(l-1)}{2l+1} \times$$

$$\times \int dr' \Omega_{\text{pr}}(r) \Omega_{\text{pr}}(r') \mathcal{F}_l(r, r') Z_l(r'). \quad (2.55)$$

For $l = 1$ one can see that $\omega^2 = 0$ satisfies this equation since $D_1^1 = \frac{1}{2}$. However, the most interesting fact consists in stability of all higher modes, $l \geq 3$. Indeed, since $1 - 2D_1^l > 0$ for $l \geq 3$, and the integral operator in the right side is positively defined, we conclude that all eigenvalues, ω^2 , are positive. Consequently, the instability is absent in the limit of circular orbits. The result is universal and does not depend on a particular choice of the model Ω_{pr} .

3 THIN DISK SYSTEMS

3.1 Integral equation for slow modes in monoenergetic model of disk

In this section we shall consider monoenergetic distributions (1.1) with even functions $f(\alpha) = f(-\alpha)$. Functions $F(E, L)$ are normalized as follows:

$$M_G = \int F d\Gamma = (2\pi)^2 \int \frac{dE}{\Omega_1(E)} \int_{-L_{\text{circ}}(E)}^{L_{\text{circ}}(E)} dL F(E, L), \quad (3.1)$$

which gives the normalization constant

$$A = \frac{M_G}{\pi^2 R^2} \quad (3.2)$$

provided that $\int_{-1}^1 f(\alpha) d\alpha = 1$.

The integral equation for slow modes (Paper I) can be represented in the form:

$$\phi(\alpha) = \frac{C_m}{\pi^3} \int_{-1}^1 \frac{d\alpha' df/d\alpha'}{\bar{\omega} - \nu(\alpha')} \mathcal{K}_m(\alpha, \alpha') \phi(\alpha'), \quad (3.3)$$

or, using the evenness of $\phi(\alpha)$ which follows from evenness of $f(\alpha)$, oddness of $\Omega_{\text{pr}}(\alpha)$, and symmetry properties of the

kernel, $\mathcal{K}_m(\alpha, \alpha') = \mathcal{K}_m(-\alpha, \alpha')$,

$$\phi(\alpha) = \frac{2C_m}{\pi^3} \int_0^1 \frac{\nu(\alpha')}{\bar{\omega}^2 - \nu^2(\alpha')} \frac{df}{d\alpha'} \mathcal{K}_m(\alpha, \alpha') \phi(\alpha') d\alpha', \quad (3.4)$$

where $\bar{\omega}$ and $\nu(\alpha)$ are dimensionless pattern speed and precession rate:

$$\bar{\omega} = \frac{\Omega_p}{\epsilon \Omega_1}, \quad \nu(\alpha) = \frac{\Omega_{pr}(\alpha)}{\epsilon \Omega_1}. \quad (3.5)$$

Changing the unknown function, integral equation (3.4) takes the form of linear eigenvalue problem:

$$[\bar{\omega}^2 - \nu^2(\alpha)] \psi(\alpha) = \frac{2C_m}{\pi^3} \int_0^1 \nu(\alpha') \frac{df}{d\alpha'} \mathcal{K}_m(\alpha, \alpha') \psi(\alpha') d\alpha'. \quad (3.6)$$

The kernel functions for thin disks $\mathcal{K}_m(\alpha, \alpha')$ can be transformed from a corresponding expression in Paper I to a suitable form as follows:

$$\mathcal{K}_m(\alpha, \alpha') = \frac{1}{C_m} \int_0^\pi d\tau r \cos m\zeta \int_0^\pi d\tau' r' \cos m\zeta' \mathcal{F}_m(r, r'), \quad (3.7)$$

where dependence of r and anomaly ζ on τ and e are the same as in the spherical case (2.8), but the function $\mathcal{F}_m(x, y)$ is

$$\mathcal{F}_m(x, y) = \int_{-\pi}^\pi \frac{\cos m\theta d\theta}{\sqrt{x^2 + y^2 - 2xy \cos \theta}}. \quad (3.8)$$

As earlier, the kernel $\mathcal{K}_m(\alpha, \alpha')$ is normalized to unity: $\mathcal{K}_m(0, 0) = 1$, which means C_m equal to

$$C_m = \int_0^1 dx \sqrt{\frac{x}{1-x}} \int_0^1 dy \sqrt{\frac{y}{1-y}} \mathcal{F}_m(x, y). \quad (3.9)$$

It immediately follows from (3.7) if one reminds that for radial orbits $\zeta = \pi$, $\cos m\zeta = (-1)^m$, $d\tau = dx [x(1-x)]^{-1/2}$. For the lowest azimuthal numbers, functions $\mathcal{F}_m(x, y)$ can be expressed through elliptical integrals of the first and the second kind $\mathbf{K}(q)$ and $\mathbf{E}(q)$:

$$\mathcal{F}_1(x, y) = \frac{4}{r_>} \frac{\mathbf{K}(q) - \mathbf{E}(q)}{q}, \quad (3.10)$$

$$\mathcal{F}_2(x, y) = \frac{4}{3r_>} \left[\left(\frac{2}{q^2} + 1 \right) \mathbf{K}(q) - 2 \left(\frac{1}{q^2} + 1 \right) \mathbf{E}(q) \right], \quad (3.11)$$

where $r_> = \max(x, y)$, $r_< = \min(x, y)$, $q = r_</r_>$. Using (3.10) and (3.11) one can obtain numerically $C_1 = 10.88$, $C_2 = 7.45$.

For the surface density we have:

$$\sigma_0(r) = \frac{2}{r} \int dE \int_{-L_{\max}(r)}^{L_{\max}(r)} \frac{F(E, L) dL}{\sqrt{2E + \frac{2GM_c}{r} - \frac{L^2}{r^2}}} = \frac{2M_G}{\pi^2 R^2} \Sigma_0(r), \quad (3.12)$$

where

$$\Sigma_0(r) = \frac{\int_{-\alpha_{\max}(r)}^{\alpha_{\max}(r)} \frac{f(\alpha) d\alpha}{\sqrt{\alpha_{\max}^2(r) - \alpha^2}}, \quad (3.13)$$

and $\alpha_{\max}^2(r) = L_{\max}^2(r)/L_{\text{circ}}^2 = 4(r/R)(1 - r/R)$ as for spheres.

Relation between the precession rate and the potential $\Phi_G(r)$ is the same as in the spherical systems, (see Tremaine 2005 and Paper I)

$$\Omega_{pr} = \frac{8}{\pi} \frac{1}{e \Omega_1 R^3} \int_0^\pi r^2 \frac{d\Phi_G}{dr} \cos \zeta d\zeta. \quad (3.14)$$

but relation between the potential and the surface density is much more complicated⁶ (see, e.g., Tremaine, 2001)

$$\Phi_G(r) = -\frac{4G}{r^{1/2}} \int (r')^{1/2} \sigma_0(r') dr' [q^{1/2} \mathbf{K}(q)]. \quad (3.15)$$

Using (3.12)–(3.15) one obtains a suitable expression for scaled precession rate $\nu(\alpha)$ (3.5) in the integral form

$$\nu(\alpha) = \alpha \int_0^1 d\alpha' f(\alpha') \mathcal{Q}(\alpha, \alpha'), \quad (3.16)$$

where $\mathcal{Q}(\alpha, \alpha')$ is a universal function for any DF:

$$\mathcal{Q}(\alpha, \alpha') = \frac{1}{\pi^3 e^2} \int_{r'_{\min}}^{r'_{\max}} \frac{r' dr'}{\sqrt{(r' - r'_{\min})(r'_{\max} - r')}} \times \int_{r_{\min}}^{r_{\max}} dr \frac{2r - \alpha^2}{r \sqrt{(r - r_{\min})(r_{\max} - r)}} \left[\frac{\mathbf{E}(\kappa)}{r' - r} - \frac{\mathbf{K}(\kappa)}{r' + r} \right]. \quad (3.17)$$

Here $\kappa = 2\sqrt{r r'}/(r + r')$. The integral from the first term is understood in the principle value sense. Using the same trick as in Sec. 2, one can change to new integrating variables τ and τ' , where $r = \frac{1}{2}(1 - e \cos \tau)$ and $r' = \frac{1}{2}(1 - e' \cos \tau')$. Then, for $\mathcal{Q}(\alpha, \alpha')$ one obtains

$$\mathcal{Q}(\alpha, \alpha') = \frac{1}{2\pi^3 e} \int_0^\pi d\tau \frac{e - \cos \tau}{1 - e \cos \tau} \int_0^\pi d\tau' (1 - e' \cos \tau') \times \left[\frac{\mathbf{E}(\kappa)}{r' - r} - \frac{\mathbf{K}(\kappa)}{r' + r} \right]. \quad (3.18)$$

3.2 Variational principle and sufficient condition for instability of $m = 1$ mode

As we saw in Sec. 2, for spherical systems with monotonic DF, the variational principle takes place. Besides, for $l = 1$ and the empty loss cone, a zero frequency solution exists which stands for a sphere displacement from the massive center; all other eigenmodes being stable. A thin disk is completely different. The displacement is no longer an eigenmode. Moreover, models with analogous distributions are

⁶ For that reason precession in the near-Keplerian disk not always retrograde.

turn out to be unstable. Let us prove the instability of lopsided $m = 1$ mode provided that

$$g(\alpha) = \nu(\alpha) df/d\alpha < 0. \quad (3.19)$$

Note that spherical models with the analogous condition are stable.

Disks with even DFs satisfying condition (3.19) obey the variational principle, which means the eigenfrequencies squared are real. So one can formulate a *sufficient* condition of instability for $m = 1$ azimuthal perturbations as follows: If the loss cone is empty ($f(0) = 0$), the DF is monotonically increasing $df/d|\alpha| > 0$, and precession is retrograde for all values of angular momentum ($\nu(\alpha)/\alpha < 0$), then $m = 1$ perturbations are unstable.

To prove the statement we use integral equation (3.4), in which we assume $\bar{\omega} = i\Gamma$ with $\Gamma > 0$:

$$\mathcal{M}(\Gamma) \phi(a) = 0, \quad (3.20)$$

where operator $\mathcal{M}(\Gamma)$ is

$$\mathcal{M}(\Gamma) \phi(a) \equiv \phi(a) + \frac{2C_m}{\pi^3} \int_0^1 \frac{g(\alpha')}{\Gamma^2 + \nu^2(\alpha')} \mathcal{K}_m(\alpha, \alpha') \phi(\alpha') d\alpha'. \quad (3.21)$$

Now we consider another eigenvalue problem

$$\mathcal{M}(\Gamma) \phi(a) = \lambda(\Gamma) \phi(a). \quad (3.22)$$

Eigenvalues Γ of the problem (3.20) correspond to eigenvalues $\lambda(\Gamma) = 0$ of the problem (3.22). Let us define an inner product as $\langle X, Y \rangle = \int_0^1 d\alpha X^*(\alpha) W(\Gamma, \alpha) Y(\alpha)$, where weight function $W(\Gamma, \alpha) = -g(\alpha)/[\Gamma^2 + \nu^2(\alpha)] > 0$. Operator \mathcal{M} has the following properties.

1. \mathcal{M} is hermitian, i.e. $\langle \psi(a), \mathcal{M}\phi(a) \rangle = \langle \mathcal{M}\psi(a), \phi(a) \rangle = \langle \phi(a), \mathcal{M}\psi(a) \rangle^*$.

2. \mathcal{M} is continuous, when $\Gamma \geq 0$. One might think that the first term $\phi(a)$ in the r.h.s. of (3.21) breaks down the continuity, which in turn means that system of proper functions is incomplete. However, this is not the case, since $\phi(a)$ can be absorbed by introducing new eigenvalue $\Lambda(\Gamma) = \lambda(\Gamma) - 1$ in (3.22). Since $f(\alpha)$ is even, for smooth DF we have $f(0) = f'(0) = 0$, $f''(0) > 0$. This condition guarantee the weight function $W(\alpha)$ to be finite even for $\Gamma = 0$, despite $\nu = \mathcal{O}(\alpha)$ at $\alpha \rightarrow 0$.

3. \mathcal{M} is positive definite at sufficiently large Γ . This is evident, since $W(\alpha) > 0$, and the second term in (3.21) becomes small at large Γ .

From the first two properties it follows that for fixed $\Gamma \geq 0$ eigenvalues $\lambda_n(\Gamma)$, $n = 1, 2, 3, \dots$ of $\mathcal{M}(\Gamma)$ are real, and the system of proper functions is complete. The third property means that at large Γ all eigenvalues $\lambda_n(\Gamma)$ are positive.

If we find a test function $\phi_t(\Gamma_0, \alpha)$, for which the scalar product $\langle \phi_t(\Gamma_0, \alpha), \mathcal{M}(\Gamma_0) \phi_t(\Gamma_0, \alpha) \rangle$ is negative, it mean $\mathcal{M}(\Gamma_0)$ is not positive definite for the given Γ_0 . So, at least one eigenvalue must be negative: $\lambda_{\min}(\Gamma_0) < 0$. This minimal eigenvalue $\lambda_{\min}(\Gamma)$ increases with Γ and becomes positive, as all other $\lambda_n(\Gamma)$. We conclude that there must be a value of Γ , $\Gamma_0 < \Gamma < \infty$ for which $\lambda_{\max}(\Gamma) = 0$. This value is an eigenvalue for (3.21), which means the existence of the eigenmode describing aperiodic instability with growth rate Γ .

For the test function $\phi_t(\Gamma_0, \alpha)$ one can take a displacement of the disk from the center, which is similar to the sphere displacement (2.15) and correspond to lopsided perturbation $m = 1$: $\phi_t(\Gamma_0, \alpha) = (e/\alpha) \nu(\alpha)$, and $\Gamma_0 = 0$. One can show that

$$\langle \phi_t(\Gamma_0, \alpha), \mathcal{M}(\Gamma_0) \phi_t(\Gamma_0, \alpha) \rangle < 0. \quad (3.23)$$

Explicitly, the l.h.s. is equal to $-P$, where

$$P = \int_0^1 d\alpha \frac{df(\alpha)}{d\alpha} \left[\frac{e(\alpha)}{\alpha} \right]^2 \nu(\alpha) + \frac{2C_1}{\pi^3} \int_0^1 d\alpha \frac{e(\alpha)}{\alpha} \times \\ \times \frac{df(\alpha)}{d\alpha} \int_0^1 d\alpha' \frac{e(\alpha')}{\alpha'} \frac{df(\alpha')}{d\alpha'} \mathcal{K}_1(\alpha, \alpha').$$

After some lengthy manipulations using (3.7), (3.10), (3.18), and condition $f(0) = 0$, one can show that P is positive, so inequality (3.23) is fulfilled.

In conclusion it is worth mention that Tremaine (2005) has also obtained a sufficient condition for a lopsided mode in the symmetrical disk using Goodman's (1988) criterion. His condition, however, differ from ours. Namely: If the loss cone is empty, $F(E, L = 0) = 0$, and $d\Phi_G(r)/dr > 0$ throughout the radial range containing most of the disk mass, then disk is unstable with respect to $m = 1$ perturbations. This formulation does not use the requirement for precession to be retrograde and the DF to be monotonically increasing, although monotonic increase of $F(E, 0) = [\partial F(E, L)/\partial L]_{L=0} = 0$, $[\partial^2 F(E, L)/\partial L^2]_{L=0} > 0$ is implied, at least for small angular momentum. Thus, the comparison between spherical and disk case can hardly be made, unless the conditions of stability is formulated in similar terms. To perform the comparison, we give our own criterion which follows directly from the integral equation.

We would like to emphasize, that the sufficient condition by Tremaine (2005) is different. Lack of the condition for the sign of precession possibly means that his criterion include two type of instability simultaneously – the radial orbit instability arising in disks with prograde precession, and the loss cone instability which require retrograde precession.

For disks composed of near-radial orbits, Tremaine's condition gives the result obtained in Paper I: a disk with symmetrical distribution $f(\alpha)$ obeying the conditions $f(0) = f'(0) = 0$, $f''(0) > 0$ is unstable if the precession is retrograde. In turn, precession of near-radial orbits is retrograde if $d\Phi_G(r)/dr > 0$.

3.3 Numerical results

To support the mathematical rationale given above and to provide a basis for possible simulations, it is useful to obtain eigenfrequencies of unstable modes for particular models. Here we consider the *power-exp* model with symmetrical distribution

$$f(\alpha) = N \frac{\alpha^2}{\alpha_T^3} \exp(-\alpha^2/\alpha_T^2), \quad (3.24)$$

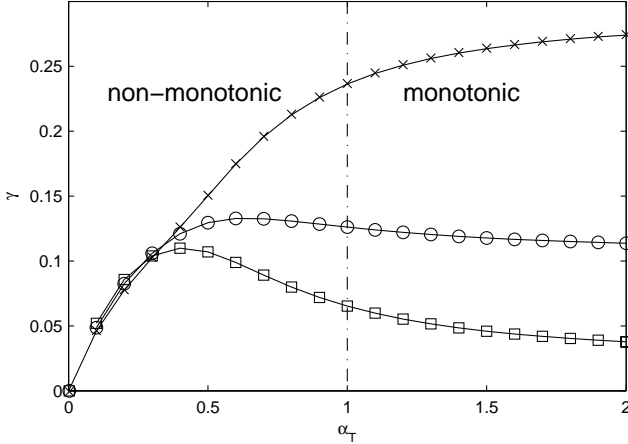


Figure 7. The dependence of the growth rates γ vs. dimensionless angular momentum dispersion α_T of initial DF for azimuthal numbers $m = 1$ (crosses), $m = 2$ (circles), and $m = 3$ (squares).

where the normalization constant is

$$N^{-1} = 2 \int_0^{1/\alpha_T^2} x^2 \exp(-x^2) dx.$$

For $\alpha_T \ll 1$ the constant $N = 2/\sqrt{\pi}$. Distributions become monotonic in the interval $[0, 1]$ when $\alpha_T \geq 1$. Note, that when $\alpha_T \gg 1$ DF is simply $f(\alpha) = \frac{3}{2}\alpha^2$ in the interval $[-1, 1]$ and doesn't depend on α_T .

Evaluation of integral equation (3.6) requires preliminary calculations of the kernel function $\mathcal{K}_m(\alpha, \alpha')$ using (3.7), and the scaled precession rate $\nu(\alpha)$ using (3.16) and (3.18). For brevity, we skip the details here, just noting that calculation of function $Q(\alpha, \alpha')$ is turn out to be rather difficult numerical task. The calculation shows that for the model (3.24) the precession rate $\nu(\alpha)$ is retrograde for all α , i.e. $\nu(\alpha)/\alpha < 0$.

The results for values of azimuthal number $m = 1, 2, 3$ are collected in Fig. 7. Since the initial distribution is symmetric, real parts of the eigenvalues $\bar{\omega}$ are equal to zero. Hence in Fig. 7 we show the imaginary parts $\gamma = \text{Im } \bar{\omega}$, which are the growth rates of the unstable modes divided by azimuthal number m , vs. dimensionless angular momentum dispersion α_T . One can see that instability exists for all α_T and never becomes saturated. Moreover, it is easy to obtain the asymptotic values γ for different m at $\alpha_T \rightarrow \infty$: 0.289, 0.108, and 0.026 for $m = 1, 2, 3$ correspondingly. For small angular momentum, growth rates increase linearly with α_T , such as γ/α_T are equal to 0.454, 0.463, and 0.481 for $m = 1, 2, 3$ correspondingly.

4 DISCUSSION

We have studied the stability of the spherically-symmetric and thin disk stellar clusters around a massive black hole. We conclude that stability properties of spherical clusters depend crucially on monotonicity of initial distribution functions, while thin disk clusters are almost always unstable.

If a initial distribution of the spherical cluster is monotonic, the cluster is most likely to be stable. This conclusion

was first made in Tremaine (2005), where stability of $l = 1$ mode was generally proved, and $l = 2$ was tested numerically. We confirm this conclusion by considering a number of monotonic distributions for modes with arbitrary l . Besides, we have checked distributions obtained from monotonic ones by making them vanish quickly but smoothly at circular orbits. These models were also stable. However, a general proof of stability for any monotonic distributions was not yet found.

Spherical clusters with non-monotonic DFs should be generally affected by the gravitational loss-cone instability. The instability was first found in our Paper I using a simplification of systems with near-radial orbits. In the Sec. 2 we show that this instability is due to just non-monotonicity of distributions over angular momentum, the orbits may not necessary be near-radial.

In our opinion, both monotonic and non-monotonic distributions are important for possible applications to real stellar clusters around black holes. The DFs monotonically increasing from the loss cone radius up to circular orbits are formed naturally due to two-body collisions of stars. It follows from numerical experiments (see, e.g., Cohn and Kulsrud, 1978) which predict establishment of such distributions after a characteristic time for collisional relaxation. These distributions may be approximated by the formula $F \propto \ln(L/L_{\min})$.

Such a slowly increasing function is, in fact, predetermined by the boundary conditions imposed in the cited numerical study and some other investigations. Indeed, a vanishing condition at $L = L_{\min}$, and a matching condition to isotropic (Maxwellian) distribution, $F = F(E)$, at the boundary $E = E_{\text{bound}} = 0$ of the phase space (E, L) (boundary separates stars which is gravitationally coupled to the black hole from the others) is required. The last condition means the asymptotic (when $E \rightarrow E_{\text{bound}}$) independence of the function $f(L)$ on the momentum L . So monotonic, or even logarithmic, dependence of type of (2.37) are quite reasonable.

The non-monotonic distributions are also real. If the cluster, is formed, for example, as a result of the collisionless collapse (several free fall times), then it remains collisionless for a long timescale of collisional relaxation. In principle, the system can have almost arbitrary DF both in the energy and in the momentum. During the collapse, a typical non-monotonic distribution of stars over the angular momentum, with empty loss cone and maximum at some value $L = L_*$, arises.

In Paper I we argued that stability properties of such a distribution is effectively analogous to typical plasma distributions of a “beam-like” form. But they can readily become unstable, as it is well-known in plasma physics (and also confirmed by direct stability study of corresponding stellar systems in Paper I). It is possible (as it is often so in plasma) that for the time of collisionless behavior, DF can undergo a dramatic changes from its initial form. In particular, the collective flux of stars into the loss cone caused by the instability could in general provide the formation of an essential part of the current mass of the black hole. Checking of such possibilities is the most urgent task for future studies of unstable *non-monotonic* models.

Since spherically-symmetric models with *monotonic* are stable apparently, but analogous disk systems are unstable

(see Tremaine 2005 and Sec. 3), a critical flatness of ellipsoid models at which the instability begins is expected. Study of such systems, as well as systems with more complex triaxial ellipsoids can be performed using numerical simulations.

ACKNOWLEDGMENTS

We are grateful to V. A. Mazur for stimulating interest in our work. The work was supported in part by Russian Science Support Foundation, RFBR grants No. 05-02-17874 and No. 07-02-00931, “Leading Scientific Schools” Grant No. 7629.2006.2 and “Young doctorate” Grant No. 2010.2007.2 provided by the Ministry of Industry, Science, and Technology of Russian Federation, and the “Extensive objects in the Universe” Grant provided by the Russian Academy of Sciences, and also by Programs of presidium of Russian Academy of Sciences No 16 and OFN RAS No 16.

REFERENCES

- Antonov V. A., 1960, *Astronomicheskii Zhurnal*, 37, 918 (in Russian)
- Antonov V. A., 1962, *Vestnik Leningr. State Univ.*, 19, 96 (in Russian)
- Antonov V. A., 1971, *Uch. zap. Leningr. State Univ.*, 359, 64 (in Russian)
- Berczik P., Merritt D., Spurzem R., 2005, *ApJ*, 633, 680
- Fridman A. M., Polyachenko V. L., 1984, *Physics of Gravitating Systems*, Springer, New York
- Kadomtsev B. B., 1966, in Leontovich M.A., ed, *Reviews of Plasma Physics: Hydromagnetic stability of a plasma*, Vol. 2. Consultants Bureau, New York, p. 153
- Kalnajs A. J., 1972, *ApJ*, 175, 63
- Cohn H., Kulsrud R. M., 1978, *ApJ*, 226, 1087
- Pal’chik M. Ya., Patashinsky A. Z., Pinus V. K., Epelbaum Ya. G., 1970, *Preprint Inst. Nucl. Phys. Sb RAS*, 99–100, Novosibirsk (in Russian)
- Polyachenko V. L., Shukhman I. G., 1972, *Preprint SibIZMIR*, No. 1-2-72. Irkutsk (in Russian)
- Polyachenko V. L., 1989, *Soviet Astron. Lett.*, 15, 385
- Polyachenko V. L., 1991, *Soviet Astron. Lett.*, 17, 371
- Polyachenko E. V., Polyachenko V. L., Shukhman I. G., 2007 (Paper I), *MNRAS*, 379, 573
- Tremaine S., 2001, *AJ*, 121, 1776
- Tremaine S., 2005, *ApJ*, 625, 143